

**Proton and cadmium adsorption by the archaeon *Thermococcus zilligii*:  
Generalising the contrast between thermophiles and mesophiles as sorbents**

Christopher J. Daughney<sup>1</sup>\*, Adrian Hetzer<sup>2</sup>†, Hannah T. M. Heinrich<sup>3,4</sup>‡, Peta-Gaye  
G. Burnett<sup>5</sup>§, Marjolein Weerts<sup>2</sup>, Hugh Morgan<sup>2</sup>, Phil J. Bremer<sup>4</sup>, A. James  
McQuillan<sup>3</sup>

<sup>1</sup> Institute of Geological & Nuclear Sciences, Lower Hutt, New Zealand

<sup>2</sup> Thermophile Research Unit, University of Waikato, Hamilton, New Zealand

<sup>3</sup> Department of Chemistry, University of Otago, Dunedin, New Zealand

<sup>4</sup> Department of Food Science, University of Otago, Dunedin, New Zealand

<sup>5</sup> Department of Soil Science, University of Saskatchewan, Saskatoon, Canada

Manuscript submitted to Chemical Geology, November 2009

---

\* Corresponding author: [c.daughney@gns.cri.nz](mailto:c.daughney@gns.cri.nz), +64-4-570-4751

† Current address: Friedrich Loeffler Institute of Medical Microbiology, University Hospital of Ernst Moritz Arndt University Greifswald, Greifswald, Germany

‡ Current address: Kraft Foods R&D Inc., Munich, Germany

§ Current address: Food and Bioproduct Sciences, University of Saskatchewan, Saskatoon, Canada

## **Abstract**

Adsorption by microorganisms can play a significant role in the fate and transport of metals in natural systems. Surface complexation models (SCMs) have been applied extensively to describe metal adsorption by mesophilic bacteria, and several recent studies have extended this framework to thermophilic bacteria. We conduct acid-base titrations and batch experiments to characterise proton and Cd adsorption onto the thermophilic archaeon *Thermococcus zilligii*. The experimental data and the derived SCMs indicate that the archaeon displays significantly lower overall sorption site density compared to previously studied thermophilic bacteria such *Anoxybacillus flavithermus*, *Geobacillus stearothermophilus*, *G. thermocatenulatus*, and *Thermus thermophilus*. The thermophilic bacteria and archaea display lower sorption site densities than the mesophilic microorganisms that have been studied to date, which points to a general pattern of total concentration of cell wall adsorption sites per unit biomass being inversely correlated to growth temperature.

**Keywords:** proton adsorption; metal adsorption; surface complexation modeling; archaea; bacteria; thermophile

## 1. Introduction

Many previous investigations have focussed on the adsorption of dissolved metals by bacteria (Fein, 2000; Fein et al., 2001; Borrok et al., 2005; Daughney and Fortin, 2006). The reactivity of bacterial cells toward dissolved metals is conferred by the cell wall functional groups (carboxyl, phosphoryl, amino, etc.), in combination with a high surface area to volume ratio and a surface electric charge that is usually negative under environmental conditions. Metal adsorption by bacteria is of interest because of its potential to influence the fate and transport of dissolved ions in natural water-rock systems.

This study extends previous work conducted with bacteria by characterising proton and metal adsorption by a member of the Domain Archaea, which to our knowledge has not been previously reported. The archaea are of interest from the perspective of metal adsorption because, like bacteria, they are ubiquitous in aquatic and geologic environments and may account for up to 20% of the biomass on earth (DeLong and Pace, 2001). Archaea were first detected in extreme environments such as hot springs (Woese and Fox, 1977), but they are now known to be widespread in soils and freshwater and marine settings as well (Hershberger et al., 1996; Bintrim et al., 1997; DeLong, 1998; Vetriani et al., 1998; DeLong and Pace, 2001). The archaea are also of interest as metal sorbents because they are phylogenetically distinct from bacteria and have a different cell wall structure (Madigan and Martinko, 2005). Peptidoglycan is the dominant bacterial cell wall component, whereas the archaeal cell wall is completely devoid of peptidoglycan and instead is made up mainly of pseudomurein or protein subunits, depending on the species. The bacterial cell wall may include teichoic acid, but its presence has not been reported in the archaeal cell wall. Bacterial cell wall phospholipids are comprised mainly of D-glycerol, generally

with ester linkages, and with fatty acid side chains without branches or rings, whereas archaeal cell wall phospholipids are comprised of L-glycerol, exclusively with ether linkages, and with isoprenoid side chains that may include multiple branches and cyclopropane or cyclohexane rings (De Rosa et al. 1986; Koga and Morii, 2005). These structural differences convey thermostability and solute impermeability to the archaeal cell wall, which are believed to be important for survival in extreme environments (Koga and Morii, 2005), and which may also influence cell wall reactivity towards protons and dissolved metals.

The experiments conducted in this study are performed with *Thermococcus zilligii*, an archaeon that was originally isolated from a freshwater hot spring in New Zealand (Klages and Morgan, 1994). Growth of *T. zilligii* is strictly anaerobic, requires sulphur and a source of organic carbon, and occurs optimally at 75-80°C (Ronimus et al., 1997). The adsorption experiments conducted in this study are based on established methods (Fein et al., 1997; Daughney et al., 1998, 2001; Yee and Fein, 2001; Haas, 2004; Borrok and Fein, 2005; Johnson et al., 2007; Ginn and Fein, 2008) in order to facilitate comparison with previous investigations. Acid-base titrations and batch adsorption experiments are used to characterise proton and metal adsorption to *T. zilligii*. Cadmium is selected as the model metal because it is a common contaminant, and because its adsorption by various mesophiles and thermophiles has been previously described (Yee and Fein, 2001; Borrok et al., 2004a; Johnson et al., 2007).

This study also aims to summarise the proton and metal adsorption properties of thermophiles as a group (optimal growth temperatures in the range 40-80°C). Most previous investigations of proton and metal adsorption by bacteria have involved mesophilic species (optimal growth temperatures in the range 20-40°C), but several

recent investigations have focussed on proton and/or metal adsorption by thermophilic bacteria (Wightman et al., 2001; Hetzer et al., 2006; Burnett et al., 2006a,b, 2007; Heinrich et al., 2007, 2008; Ginn and Fein, 2008; Lalonde et al., 2008; Tourney et al., 2008; Özdemir et al., 2009). Surface Complexation Models (SCMs) have been developed to describe proton and metal adsorption by both thermophilic and mesophilic bacteria, and can provide a framework for assessing any differences that might exist in the adsorptive properties of the two groups, through comparison of model parameters. The SCMs previously developed to describe proton and metal adsorption by thermophilic bacteria do seem to reveal certain general contrasts to the so-called “universal” SCMs for proton and metal adsorption for mesophilic bacteria (Yee and Fein, 2001; Borrok et al., 2005; Johnson et al., 2007).

However, previously published SCMs for proton and/or metal adsorption by bacteria have employed different assumptions, and so a direct comparison of model parameters for individual species or consortia is not straight forward. Most previously published SCMs have incorporated reactions of the following types to describe proton and metal adsorption, respectively, by cell wall functional groups:



where  $R$  represents the cell wall, attached to which are  $n$  different types of functional groups  $L_n$  with charge  $x$  when protonated, and  $M$  represents a metal ion with charge  $y$ . Fitting of the SCM to the experimental data involves determination of the site concentrations and stability constants  $K$  for deprotonation of and metal adsorption by each different type of functional group:

$$K_H^n = \frac{[R - L_n^{x-1}] a_{H^+}}{[R - L_n H^x]} \quad (3)$$

$$K_M^n = \frac{[R - L_n M^{x+y-1}]}{[R - L_n^{x-1}] a_{M^y}} \quad (4)$$

where square brackets represent the concentration of the enclosed cell wall surface species and  $a$  represents the activity of the subscripted aqueous species. The number of different types of surface sites employed in previous SCMs varies from one to four (but proton and metal adsorption are almost always assumed to follow a 1 to 1 stoichiometry). In some models, there is assumed to be a discrete value for each stability constant (e.g. Fein et al., 1997), whereas other models invoke an affinity spectrum approach (e.g. Cox et al., 1999). “Non-electrostatic” models do not account for the effect of the cell surface electric field on proton or metal adsorption (e.g. Borrok et al., 2005; Johnson et al., 2007), whereas “electrostatic” models involve adjustment of stability constants as follows:

$$K^{\text{int}} = K \exp(-ZF\psi / RT) \quad (5)$$

where  $K^{\text{int}}$  is the intrinsic stability constant referenced to zero surface charge and zero surface coverage, and the variables  $Z$ ,  $F$ ,  $\psi$ ,  $R$  and  $T$  refer to the charge of the adsorbing ion, Faraday’s constant, the electric potential at the location of adsorption, the gas constant and the absolute temperature, respectively. Various electric double layer models have been integrated into SCMs to determine the electric potential of the cell surface, including the constant capacitance model (Fein et al., 1997; Daughney et al., 1998; Ngwenya et al., 2003), the Stern model (Daughney and Fein, 1998), the diffuse layer and triple layer models (Borrok and Fein, 2005) and the Donnan model (Yee et al., 2004, Burnett et al., 2006a,b; Heinrich et al., 2007, 2008).

In this study, we follow the approach of Borrok et al. (2005) and use a consistent modelling framework to re-develop SCMs for proton and Cd adsorption by the archaeon *T. zilligii* and previously studied thermophilic bacteria (Wightman et al.,

2001; Hetzer et al., 2006; Burnett et al., 2006a,b, 2007; Heinrich et al., 2007, 2008; Ginn and Fein, 2008; Tourney et al., 2008). The same SCM framework is employed to re-develop universal SCMs for proton and Cd adsorption by mesophilic bacteria (Yee and Fein, 2001; Borrok et al., 2005; Johnson et al., 2007). SCM model parameters are then compared for uniform conditions of pH, ionic strength and sorbate-to-biomass ratio, with the aim of identifying and quantifying any significant and systematic differences between mesophiles and thermophiles.

## **2. Materials and methods**

### **2.1 Preparation of archaeal suspensions**

*T. zilligii* strain AN1 (DSM 2270) was grown under anaerobic conditions in 800 ml of medium (5% inoculum volume) at 75°C without agitation. The medium contained (per litre): 8.00 g of trypticase peptone, 2.50 g of NaCl, 1.50 g of KH<sub>2</sub>PO<sub>4</sub>, 1.00 g of sodium thioglycollate, and 4.00 g of L-cystine. L-cystine was dissolved at double-strength (8.00 mg/l) in boiling water at pH 12 prior to addition to the medium. The medium was adjusted to the final pH value of 7.4 and autoclaved anaerobically under a nitrogen atmosphere. Cells were harvested after 36 h incubation in the middle of the exponential growth phase, at a culture optical density at 600 nm (OD<sub>600</sub>) of roughly 0.2, by centrifugation at 1,850g. Cells were washed five times in 250 ml 0.01 M NaNO<sub>3</sub> to guarantee complete removal of the growth medium. After the final wash, the cell pellet was resuspended in a known weight of 0.01 M NaNO<sub>3</sub> and OD<sub>600</sub> was measured relative to the electrolyte.

Biomass concentrations in the cell suspensions were determined using several methods. Aliquots of cell suspension were weighed and then centrifuged at 1,850g for one hour, stopping at 20 minute intervals to decant the supernatant, whereupon the

final wet weight of the cell pellet was determined. The dry mass of the cell pellet was determined after drying at 80°C to constant weight. The relationships between wet and dry biomass concentrations and optical density were established by measuring OD<sub>600</sub> of washed cell suspensions. Total cell numbers were measured by counting in a Thoma counting chamber (depth 0.02 mm) under phase-contrast microscopy. Assessments of biomass concentration were performed on three individual cell cultures to determine inter-culture variability.

Cell dimensions were obtained using scanning electron microscopy. Cells were captured onto a 0.22 µm filter and fixed in 2.5% glutaraldehyde. The filter was exposed to four changes of 0.1 M sodium cacodylate buffer. After sequential dehydration in an increasing concentrations of ethanol (50%, 75%, 90%, and absolute ethanol), the filter was dried at the critical point, sputtered with platinum, and examined using a Hitachi S-4100 field emission scanning electron microscope.

## **2.2 Acid-base titrations**

A known weight (40–50 g) of cell suspension (2.5–8.5 dry g per litre, containing the combined biomass from between 4 and 19 individual cultures) was transferred into an air-tight polystyrene vessel. The pH was adjusted to roughly 3.5 by the addition of a known volume of standardized 0.1 M HNO<sub>3</sub>, and the suspension was mixed with an overhead magnetic stirrer and bubbled with humid CO<sub>2</sub>-free N<sub>2</sub> gas for 30 min, to remove dissolved CO<sub>2</sub> from the suspension. The titration was conducted in an up-pH direction to pH 10 at 22 ± 1°C using standardized CO<sub>2</sub>-free 0.1 M NaOH and a Mettler DL 22 autotitrator. Throughout the duration of the titration, the suspension was continually stirred and bubbled with N<sub>2</sub> gas. Following each addition of titrant, the pH of the suspension was recorded when a stability criterion of 5



mV/min was obtained. After the completion of the first up-pH titration, the suspension was acidified to roughly pH 3.5, and a second up-pH titration was performed to investigate the reversibility of proton adsorption. The reproducibility of the experimental method was evaluated by performing duplicate titrations of two separate aliquots (ca. 50 g) of a single parent suspension. The total volume of acid and base added, relative to the initial volume of the suspension, was such that the maximum dilution was less than 10% (accounted for in modelling of the data). The entire procedure was conducted with four independently prepared parent suspensions, to examine inter-culture variability. Control titrations of the electrolyte alone were performed on a regular basis to test for infiltration of CO<sub>2</sub> into the titrants and the experimental apparatus.

### **2.3 Cadmium adsorption experiments**

*T. zilligii* cells were cultured, rinsed and resuspended in 0.01 M NaNO<sub>3</sub> as described above, OD<sub>600</sub> was measured to determine biomass concentration, and then three dilutions of the cell suspension were prepared in 0.01 M NaNO<sub>3</sub>, having 100%, 50% and 25% the biomass concentration of the parent suspension. Known weights of the three diluted suspensions were then spiked with 1000 ppm cadmium atomic absorption standard solution (Merck, Cd(NO<sub>3</sub>)<sub>2</sub> in 0.5% HNO<sub>3</sub>) to a final yield a concentration of 5 ppm cadmium. All three cell suspensions were examined by phase-contrast microscopy to check cell integrity. Each of the three cadmium-spiked cell suspensions was then divided into 5 ml aliquots and transferred into 8 to 10 individual test tubes. The pH of each test tube was adjusted by adding small volumes of 0.1 M NaOH solution, to cover the pH range of roughly 3.5 to 8 for each of the three dilutions of the parent cell suspension. The test tubes were equilibrated in an orbital

mixer incubator set at 100 rpm and 22°C. Following equilibration, the samples were centrifuged at 1,850g for 10 minutes. An aliquot of the supernatant was decanted and acidified with concentrated HNO<sub>3</sub> solution (ARISTAR grade) for subsequent cadmium analysis by flame atomic absorption spectroscopy (GBC Avanta). The remaining supernatant was used for measurement of final equilibrium pH. In an initial experiment to assess the kinetics of cadmium adsorption, the equilibration time was varied (10 min to 120 min in 10 min intervals, 180 min, and 240). The kinetic experiment indicated that equilibration occurred within the first 120 minutes, and thus 120 minutes was used as the equilibration time for all subsequent experiments. The concentration of cadmium adsorbed by the cells in each sample was calculated by subtracting the cadmium ion concentration remaining in the supernatant (determined by atomic absorption spectroscopy) from the original concentration of 5 ppm. The entire procedure was conducted with four independently prepared parent suspensions, to examine inter-culture variability. Control experiments involving Cd in the electrolyte but without *T. zilligii* cells were performed to test for Cd precipitation and/or adsorption to the experimental apparatus. Control experiments involving biomass in electrolyte without added Cd were conducted to test for Cd release from *T. zilligii* cells.

## **2.4 Surface Complexation Modelling**

SCMs were constructed using FITMOD (Daughney et al., 2004), a modified version of the computer program FITEQL 2.0 (Westall, 1982). All SCMs developed in this study include equilibria describing the dissociation of water, the acid, the base, and the electrolyte. SCMs for Cd adsorption also incorporate reactions for Cd hydrolysis and Cd complexation by carbon dioxide, with stability constants taken

from the Critical Stability Constants Database (Smith and Martell, 1976). All stability constants are adjusted for ionic strength using the Davies equation (Langmuir, 1997), and all values tabulated in this paper are referenced to zero ionic strength and 25°C.

SCMs were used for three purposes in this investigation. Firstly, SCMs were used to derive model curves for proton and metal adsorption by previously studied mesophilic and thermophilic species and consortia. This was achieved by using previously published SCM parameters and configurations (e.g. number of sites, electrostatic double layer model, etc.), without modification or optimisation. The only adjustment to the previously published SCMs was to generate the predictions for uniform conditions to enable meaningful comparison. The selected conditions for comparison were biomass concentration of 1 wet gram per litre, ionic strength of 0.01 M, and, for simulations involving Cd adsorption, a total Cd concentration of  $5 \times 10^{-5}$  M. These conditions for the comparison were selected because they are representative of the experimental conditions used in most previous studies, and hence the published SCM parameters were not being used to extrapolate proton and/or Cd adsorption too far outside the range used for the original model calibration. SCM values of the initial proton condition ( $T_H^0$ , cf. Westall et al., 1995; Fein et al., 2005) were included in the modelling where available. Comparison of SCM curves that did or did not consider the initial proton condition was achieved by evaluating the change in adsorption over the pH range of interest, as opposed to the absolute amount of adsorption.

Secondly, SCMs were developed in this study to describe proton and Cd adsorption by *T. zilligii*. The SCMs developed for this purpose were based on a discrete site, non-electrostatic approach in order to permit comparison to the widest range of previous investigations (many previous investigations did not report all of the necessary information to enable application of an electrostatic modelling approach).

Fitting of the model to the experimental data involved optimising the total concentration of each type of surface site and the values of the stability constants describing proton and metal adsorption (Equations 3 and 4). Model fit was quantified using the overall variance  $V(Y)$  reported by FITMOD, where  $Y$  represents the difference in the total proton or metal mass balance calculated from the model in comparison to the experimental data, weighted for experimental uncertainty and the number of degrees of freedom in the model optimisation (Westall, 1982; Heinrich et al., 2008). The ideal value for  $V(Y)$  is 1, indicating that the error in the model is equal to the estimated uncertainty in the experimental data. Lower numbers indicate that the model contains too many adjustable parameters or that the error estimates are too large, whereas numbers much higher than 1 indicate a poor fit to the data. Generally a value of  $V(Y)$  between 1 and 20 is considered an indication of adequate model fit to a single experimental dataset (Westall, 1982), whereas an adequate fit to data from several different experiments, particularly for independent cultures of bacteria, can be indicated by  $V(Y)$  up to ca. 50 (Burnett et al., 2007). Confidence intervals for  $V(Y)$  were calculated as described by Heinrich et al. (2008):

$$\frac{V(Y) \times (n_P \times n_Q - n_R)}{\chi_{1-\alpha/2}^2}, \quad \frac{V(Y) \times (n_P \times n_Q - n_R)}{\chi_{\alpha/2}^2} \quad (6)$$

where  $n_P$ ,  $n_Q$  and  $n_R$  represent the number of data points, the number of components for which both free concentration and total concentration are known, and the number of parameters being optimised, respectively, and  $\chi_p^2$  is the quantile of the chi-square distribution having  $(n_P \times n_Q - n_R)$  degrees of freedom with exceedence probability  $p$ . For this study,  $V(Y)$  values of different models were considered significantly different when their 95% confidence intervals did not overlap.

Thirdly, in this study we follow the approach of Borrok et al. (2005) and re-develop SCMs using a consistent modelling framework to describe proton and Cd adsorption by the archaeon *T. zilligii* and previously studied mesophilic and thermophilic bacteria (Wightman et al., 2001; Yee and Fein, 2001; Borrok et al., 2005; Hetzer et al., 2006; Burnett et al., 2006a,b, 2007; Johnson et al., 2007; Heinrich et al., 2007, 2008; Ginn and Fein, 2008). This involves using the previously published SCMs to predict proton and Cd adsorption for standard conditions as described above (1 g wet biomass per litre, 0.01 M ionic strength,  $5 \times 10^{-5}$  M total Cd) at increments of 0.25 pH units from pH 3 to 10, and then fitting a new three-site non-electrostatic SCM to the resulting dataset. This ensures that the re-developed SCMs all employ the same model assumptions, cover the same chemical conditions, and are all based on the same number of data points, such that meaningful comparisons can be made between the SCM parameters for different species and consortia. This approach of re-developing previously published SCMs is justified for the aim of this study, i.e. comparison of the adsorptive properties of thermophiles and mesophiles, because several studies have shown that various types and configurations of electrostatic and non-electrostatic SCMs can provide a good fit to experimental data for proton and metal adsorption by bacteria (Daughney and Fein, 1998; Borrok and Fein, 2005; Fein et al., 2005). For example, some of the previously published SCMs invoke four different types of surface sites, but may cover a broader range of pH than we employ for the comparisons made in the present investigation. The suitability of the three-site modelling approach used in this study is indicated by the fact that all of the re-developed SCMs possess  $V(Y)$  values that are statistically indistinguishable from the ideal value of 1, meaning that the re-developed three-site non-electrostatic SCMs would fit the original experimental data as well as the originally published SCMs for

the pH range from 3 to 10. For the pH range and experimental conditions considered in the present study, four-site models either did not converge or did not offer statistically significant improvement in fit compared to the three-site models.

### **3. Results and Discussion**

#### **3.1 Characteristics of *T. zilligii* cells**

After 36 h incubation time, *T. zilligii* populations were in mid-exponential growth phase (growth curves not shown). Examination by optical and scanning electron microscopy indicated that the cells were intact, and had coccoid shape and diameter roughly 1  $\mu\text{m}$ , in agreement with Ronimus et al. (1997). Assessments of biomass concentration showed that  $\text{OD}_{600} = 1.000$  corresponded to  $5.0 \times 10^8$  cells per ml and 0.329 g dry biomass per litre. The ratio of wet to dry biomass was determined to be 11.1 to 1. These characteristics of *T. zilligii* cells are comparable to other microorganisms for which SCMs have been developed (Fein et al., 1997; Wightman et al., 2001; Yee et al., 2004; Burnett et al., 2006a; Hetzer et al., 2006; Heinrich, 2008).

#### **3.2 Proton adsorption by *T. zilligii***

The experimental titration data show that *T. zilligii* cell suspensions possess substantial buffering capacity over the range from pH 3 to 10 (Figure 1). Buffering capacity increases with the weight of cells present (Figure 1a), but the data show good agreement when normalised to biomass concentration (Figure 1b). There is excellent agreement between the first and second titrations of a single aliquot cell suspension (indicated by points of the same shape on Figure 1), indicating that proton adsorption/desorption reactions are rapid and reversible on the time scale of these

experiments (ca. 1 h). Control titrations indicated that the electrolyte alone possessed negligible buffering capacity (data not shown), and hence the buffering capacity observed for *T. zilligii* cell suspensions is inferred to arise from desorption of protons from cell surface functional groups. Several previous studies conducted with mesophilic and thermophilic bacteria have reported similar results, with buffering capacity of cell suspensions observed to be reversible, reproducible and similarly related to pH and biomass concentration (Fein et al., 1997; Daughney and Fein, 1998; Daughney et al., 1998, 2001; Cox et al., 1999; Yee and Fein, 2001; Borrok et al., 2005; Fein et al., 2005; Burnett et al., 2006a; Hetzer et al., 2006; Heinrich et al., 2007, 2008).

The titration datasets were modelled using FITMOD and non-electrostatic, discrete site SCMs (Figure 1b, Table 1). When data from the four individually prepared cell suspensions were modelled separately, SCMs that incorporate only two types of surface sites yielded  $V(Y)$  values in excess of the acceptable threshold of 20 for two of the datasets, indicating relatively poor fit to the data. SCMs that incorporate three types of surface sites offer improved fits to three of the individual datasets, with convergence not being achieved for the dataset with the highest biomass concentration. Non-convergence is an indication that the additional type of surface site in the model is not warranted by the experimental data, and appropriate model configuration is known to depend on biomass concentration, pH range and so on (e.g. Daughney et al., 1998). SCMs incorporating four different types of surface sites either fail to converge or do not offer significant improvement in fit relative to the three-site models. The three-site SCM also provides the best fit when the data from all four individual titrations are modelled simultaneously (Table 1). Hence we conclude that SCMs that incorporate three distinct types of surface sites are most

appropriate for the data obtained from titration of *T. zilligii* cell suspensions, although we acknowledge that the number of sites required to fit the data is controlled to some extent by the SCM framework employed and the pH range of the titration.

The three-site SCM that provides the best fit to all of the titration data has  $V(Y) = 13.6$  (95% confidence limits for  $V(Y)$  are 11.8 to 15.8), with  $pK_a$  values for the sites being  $4.60 \pm 0.21$ ,  $6.26 \pm 0.38$  and  $8.96 \pm 0.14$ , and the respective site concentrations (in  $10^{-5}$  mol per gram wet biomass) being  $2.51 \pm 0.81$ ,  $2.51 \pm 0.21$  and  $2.51 \pm 1.26$  (uncertainties in  $pK_a$  values and site concentrations represent  $1\sigma$  values derived from modelling the four datasets independently). Based on the magnitudes of the modelled  $pK_a$  values, we speculate that the *T. zilligii* surface sites correspond to carboxyl, phosphoryl and amino functional groups, as observed in previous investigations of Gram-positive and Gram-negative bacteria.

Specific studies of the cell wall composition of *T. zilligii* are not available, but structural inferences can be based on descriptions for other *Thermococci* (Madigan and Martinko, 2005). Like other *Thermococci*, the *T. zilligii* cell wall is likely dominated by pseudomurein (without peptidoglycan or teichoic acid), which would likely reduce the concentration of phosphoryl groups in particular and probably also carboxyl groups relative to the bacterial cell wall. Sulphate groups may be present in the carbohydrate cell walls of the halophilic archaea but unlikely to be present in the cell wall of *Thermococci*. Krader and Emerson (2004) have inferred the presence of an S-layer of crystalline protein outside the cell wall of several *Thermococci*, and although *T. zilligii* was not specifically investigated, it may also have an S-layer, which may contribute additional amino groups without restricting the access of ions to cell wall functional groups. Spectroscopic analysis would be required to confirm the presence or absence of specific functional groups in the cell wall of *T. zilligii*.



### 3.3 Cd adsorption by *T. zilligii*

Control experiments indicated negligible loss of Cd from solution in the absence of *T. zilligii* cells (data not shown). In the presence of *T. zilligii* cells, Cd adsorption increases with increasing biomass concentration and increasing pH (Figure 2 displays data from a representative cell suspension). Similar patterns of dependence of metal adsorption on biomass-to-sorbate ratio and pH have been observed for many species of mesophilic and thermophilic bacteria (Fein et al., 1997; Daughney and Fein, 1998; Daughney et al., 1998; Fowle and Fein, 1999; Daughney et al., 2001; Yee and Fein, 2001; Ngwenya et al., 2003; Borrok et al., 2004a,b, 2005; Hetzer et al., 2006; Burnett et al., 2006b, 2007; Johnson et al., 2007; Ginn and Fein, 2008). Hence, as inferred for metal adsorption by bacteria, the patterns of Cd adsorption observed for *T. zilligii* likely arise from interactions between Cd and functional groups on the cell surface, and the extent of adsorption is enhanced by an increase in the biomass-to-Cd concentration ratio and by reduction in the competition between  $\text{Cd}^{2+}$  and  $\text{H}^+$  ions (as pH increases).

The Cd adsorption datasets were modelled using FITMOD and non-electrostatic, discrete site SCMs (Figure 2, Table 2). The SCMs developed to fit the Cd adsorption data incorporate three distinct types of surface functional groups, using the best-fitting  $\text{p}K_a$  values and site concentrations derived from the titration data (Table 1). Data from each of the four independently prepared cell suspensions can be adequately matched by SCMs that invoke adsorption of  $\text{Cd}^{2+}$  onto only one type of surface functional group (1:1 stoichiometry). The best fit is obtained for  $\text{Cd}^{2+}$  adsorption onto the functional group having  $\text{p}K_a = 4.60$ . SCMs that consider  $\text{Cd}^{2+}$  adsorption onto any combination of two or three different types of surface sites do not

converge (results not tabulated), indicating that inclusion of the additional reaction mechanisms are not warranted by the experimental data. When data from all four Cd adsorption experiments are modelled simultaneously, again the best fitting SCM is based on adsorption of  $\text{Cd}^{2+}$  onto only one type of surface site, namely that having  $\text{p}K_{\text{a}} = 4.60$  (Table 2). Several previous studies involving mesophilic and thermophilic bacteria have developed similar SCMs, i.e. with inclusion of reactions for proton adsorption onto three different types of surface sites but metal adsorption onto only one type of surface site (Fein et al., 1997; Daughney and Fein, 1998; Daughney et al., 1998, 2001; Yee et al., 2001; Burnett et al., 2006a; Hetzer et al., 2006). However, we acknowledge that the number and type of reaction sites required to fit the data is controlled by the SCM framework employed and the range of pH and biomass-to-Cd concentration ratio used in the experiments, such that spectroscopic evidence is required to determine the chemical environment of the bound metal and the identity of the surface site(s) involved.

### **3.4 Comparison of thermophiles and mesophiles as sorbents**

Proton adsorption by mesophilic bacteria has been generalised by Borrok et al. (2005), who developed a universal non-electrostatic SCM based on experimental titration data for 36 different individual species and consortia. This universal SCM for proton adsorption by mesophilic bacteria incorporates four different types of surface sites with  $\text{p}K_{\text{a}}$  values of 3.1, 4.7, 6.6 and 9.0 and a total site concentration of  $3.2 \pm 1.0$  ( $1\sigma$ ) moles per gram wet biomass. Figure 3 displays the expected buffering capacity as a function of pH for a suspension of mesophilic bacteria having biomass concentration of 1 wet g per litre, based on the model of Borrok et al. (2005). The universal model of Borrok et al. (2005) is plotted in Figure 3 corresponding to a

reasonable upper bound for growth temperature of 37°C, but note that the model is based on cultures with a range of growth temperatures, including some datasets for which growth temperature is unknown. Borrok et al. (2005) concluded that ionic strength, temperature and growth conditions have relatively little influence on proton adsorption by mesophilic bacteria, and hence these factors are ignored in the universal SCM, but feature into determination of the 1 $\sigma$  error bounds displayed in Figure 3. Universal SCMs for proton adsorption by mesophilic bacteria have also been developed by Yee and Fein (2001) for laboratory-maintained cultures grown at 32°C and by Johnson et al. (2007) for field consortia cultured at room temperature (inferred to be 25°C), both of which yield model curves that are comparable to the SCM derived by Borrok et al. (2005).

Proton adsorption characteristics of previously studied thermophilic bacteria are generally similar to each other, but all of the thermophiles possess relatively low adsorptive capacity per unit wet biomass compared to mesophilic bacteria (Figure 3). One possible exception is for the thermophile *B. licheniformis* S-86, which when cultured at 30°C has a similar buffering capacity to the universal mesophilic SCM of Borrok et al. (2005) (Tourney et al., 2008; unknown wet-to-dry weight ratio prevents plotting of a model curve for *B. licheniformis* S-86 data in Figure 3). Model curves for proton adsorption by thermophilic bacteria in stationary phase generally fall near or just outside the lower 1 $\sigma$  bound for mesophiles, but thermophilic populations in exponential phase display greater buffering capacity that is similar to the universal SCM from Borrok et al. (2005). Heinrich et al. (2008) have concluded that variations in buffering capacity as a function of growth time may be caused by loss of cell wall integrity, partial cell wall hydrolysis and/or other factors which may differ between species and may depend on the experimental protocols used. *T. zilligii* in exponential

phase displays lower buffering capacity per unit wet biomass than any of the thermophilic bacteria that have been studied to date, which may be the result of differences in the cell wall structure of archaea relative to bacteria, although future studies with other archaea are required to test this hypothesis.

The influence of growth temperature on buffering capacity by microorganisms can be summarised by comparing the total proton adsorption occurring for different species at a biomass concentration of 1 wet g per litre and over the pH range 4 to 10 (Figure 4). The pH range from 4 to 10 is selected for this comparison because it is covered by all previous investigations, and exclusion of data from lower and higher pH values avoids the possibility that some portion of the buffering observed for some species under more acidic or alkaline conditions is the result of cell wall damage or the production of exudates (compare Claessens et al., 2004; Fein et al., 2005; Claessens et al., 2006). The previously published SCMs for individual species and consortia have been developed from experiments conducted at ionic strength of 0.01 or 0.1 M, and it is assumed that these differences in ionic strength would have relatively little influence on the general trends displayed in Figure 4 (Daughney and Fein, 1998; Borrok and Fein, 2005; Borrok et al., 2005, Burnett et al., 2006a). The comparison of buffering capacity depicted in Figure 4 indicates that the three previously published universal SCMs for mesophilic bacteria are all comparable (Yee and Fein, 2001; Borrok et al., 2005; Johnson et al., 2007), and that the total adsorptive capacity per unit biomass of thermophiles as a group is lower than that of mesophiles as a group, based on the species and consortia that have been studied to date.

Universal SCMs have also been developed to describe Cd adsorption by mesophilic bacteria (Yee and Fein, 2001; Johnson et al., 2007). Figure 5 displays the expected extent of adsorption as a function of pH for a suspension of having  $5 \times 10^{-5}$

M total Cd and a concentration of 1 wet g mesophilic bacteria per litre, based on the universal SCM of Yee and Fein (2001) (shaded area represents  $1\sigma$  uncertainty bounds). The SCM of Yee and Fein (2001) was developed from experiments conducted at an ionic strength of 0.1 M, but the model curves depicted in Figure 5 are extrapolated to an ionic strength of 0.01 M to enable comparison with other studies. This extrapolation of the universal SCM from 0.1 M to 0.01 M ionic strength is reasonable because whilst Cd adsorption by bacteria is known to be sensitive to change in ionic strength over this range 0.01 to 0.5 M (Daughney and Fein 1998; Borrok and Fein, 2005), the influence of ionic strength can be predicted with the universal SCM because it is likely dominantly related to changes in the aqueous activity of Cd and not due to electrostatic effects related to the cell surface charge (Borrok and Fein, 2005). The universal SCM for Cd adsorption by mesophilic consortia published by Johnson et al. (2007) yields model curves that are similar to those of Yee and Fein (2001).

Compared to mesophilic bacteria, previously studied thermophiles possess relatively low Cd adsorption capacity per unit biomass (Figure 5). As observed for proton adsorption, the model curves for Cd adsorption by thermophilic bacteria fall near or just outside the lower  $1\sigma$  bound for mesophiles. Few previous investigations have assessed Cd adsorption as a function of growth phase, and so its possible influence cannot be adequately determined. *T. zilligii* in exponential phase displays lower Cd adsorption capacity per unit biomass than any of the thermophilic bacteria that have been studied to date, which mirrors the pattern observed for proton adsorption. The lower Cd adsorption may be the result of differences in the cell wall structure of the archaea relative to bacteria, although future studies with other archaea are required to test this hypothesis.

The influence of growth temperature on Cd adsorption by microorganisms can be summarised by comparing the total Cd adsorption that occurs for different species at pH 6, ionic strength of 0.01 M, and total concentrations of  $5 \times 10^{-5}$  M Cd and 1 wet g wet biomass per litre (Figure 6). These conditions are selected for the comparison because they are typical of the experimental conditions used in most previous studies, and hence the previously published SCMs are expected to be valid. As observed for the general comparison of proton adsorption, the comparison of Cd adsorption shown in Figure 6 indicates that the two previously published universal SCMs for mesophilic bacteria are comparable (Yee and Fein, 2001; Johnson et al., 2007), and that the total adsorptive capacity per unit biomass of thermophiles as a group is lower than that of mesophiles as a group. Comparisons made for other values of pH or Cd-to-biomass concentration ratio yield similar general results.

The general result of the analyses described above is that thermophiles have lower capacity to adsorb protons and Cd per unit wet biomass when compared to mesophiles. It is known that changes in growth temperature may lead to changes in cell wall structure and fluidity (e.g. Fernández Murga et al., 2000; Kremer et al., 2002). However, it is not possible to use the information presented in Figures 3 to 6 to detect more subtle variations in adsorptive properties, such as differences in  $pK_a$  values or relative proportions of surface sites, because previous studies have employed different SCM frameworks, yielding model parameters that are not directly comparable. We therefore use a consistent three-site non-electrostatic SCM framework to re-develop models for the various datasets shown in Figures 3 to 6. We acknowledge that the re-developed three-site non-electrostatic SCMs cannot match all types of previously published information, such as electrophoretic mobilities (e.g.

Burnett et al., 2006a; Heinrich et al., 2007); the intent here is to limit the comparison to the SCM parameters for proton and metal adsorption.

Model parameters for the re-developed three-site non-electrostatic SCMs are given in Table 3. The Kruskal-Wallis test indicates that there is no difference between the mesophiles and thermophiles in terms of  $pK_a$  values for Site 1 or Site 2 ( $p > 0.1$ ), but the  $pK_a$  values for Site 3 are significantly lower for the thermophiles ( $p < 0.05$ ). The total concentration of surface sites is significantly less for the thermophiles, which is almost entirely due to a lower concentration of Site 1 ( $p < 0.05$ ). There are no significant differences in  $\log K$  values for Cd adsorption by thermophiles compared to mesophiles ( $p > 0.1$ ). Hence, the lesser proton and Cd adsorption to thermophiles compared to mesophiles (Figures 3 to 6) appears to derive mainly from lower concentrations of Site 1 (i.e. the site with  $pK_a$  value approximately 4.0), rather than differences in the concentrations of other sites or differences in stability constants for proton or Cd adsorption. It must be stressed that the re-developed SCMs are used here simply for the basis of comparison of model parameters for proton and Cd adsorption between different species and consortia, and not to infer the actual reaction mechanisms that may be occurring during adsorption; future spectroscopic evidence would be essential for the latter purpose.

#### **4. Conclusions**

This study extends previous work focussed on mesophilic and thermophilic bacteria by assessing proton and metal adsorption by the thermophilic archaeon *T. zilligii*. Proton and metal adsorption by *T. zilligii* is shown to be rapid and strongly dependent on pH and metal-to-biomass concentration ratio, but occurs to a lesser extent than for the bacteria that have been studied to date. The thermophilic bacteria

as a group appear to have broadly similar adsorptive characteristics, but generally have lower adsorptive capacity per unit biomass compared to the mesophiles. This may point to a general pattern of total concentration of cell wall adsorption sites per unit biomass being inversely correlated to growth temperature, although further studies would be required to confirm this hypothesis. The thermophilic archaeon *T. zilligii* has lower adsorptive capacity per unit biomass than any other thermophile studied to date, which may reflect differences in cell wall structure between the archaea and bacteria. This study has also shown that previously published electrostatic SCMs can be re-developed effectively using a non-electrostatic framework, confirming that it is possible to fit a single dataset with more than one SCM configuration.

### **Acknowledgements**

Research funding was provided by the New Zealand Foundation of Research, Science & Technology (Contract Number C05X0303: Extremophilic Microorganisms for Metal Sequestration from Aqueous Solutions). Helen M. Turner (University of Waikato) is thanked for assistance with SEM micrographs. Associate Editor Jeremy Fein and two anonymous reviewers are thanked for their insightful suggestions for improvement of this manuscript.



## References

- Bintrim, S.B., Donahue, T.J., Handelsman, J., Roberts, G.P., Goodman, R.M., 1997. Molecular phylogeny of Archaea from soil. *Proc. Nat. Acad. Sci. USA* 94, 277-282.
- Borrok, D., Fein, J.B., 2005. The impact of ionic strength on the adsorption of protons, Pb, Cd, and Sr onto the surfaces of Gram negative bacteria: testing non-electrostatic, diffuse, and triple-layer models. *J. Coll. Interface Sci.* 286, 110-126.
- Borrok, D., Fein, J.B., Kulpa, C.F., 2004a. Proton and Cd adsorption onto natural bacterial consortia: Testing universal adsorption behaviour. *Geochim. Cosmochim. Acta* 68, 3231-3238.
- Borrok, D., Fein, J.B., Kulpa, C.F., 2004b. Cd and proton adsorption onto bacterial consortia grown from industrial wastes and contaminated geologic settings. *Environ. Sci. Technol.* 38, 5656-5664.
- Borrok, D., Turner, B.J., Fein, J.B., 2005. A universal surface complexation framework for modeling proton binding onto bacterial surfaces in geologic settings. *Am. J. Sci.* 305, 826-853.
- Burnett, P., Heinrich, H., Peak, J.D., Bremer, P.J., McQuillan, A.J., Daughney, C.J., 2006a. The effect of pH and ionic strength on proton adsorption by the thermophilic bacterium *Anoxybacillus flavithermus*. *Geochim. Cosmochim. Acta* 70, 1914-1927.
- Burnett, P., Daughney, C.J., Peak, J.D., 2006b. Cd adsorption onto *Anoxybacillus flavithermus*: surface complexation modeling and spectroscopic investigations. *Geochim. Cosmochim. Acta* 70, 5253-5269.

- Burnett, P.-G.G., Handley, K., Peak, D., Daughney, C.J., 2007. Divalent metal adsorption by the thermophile *Anoxybacillus flavithermus* in single and multi-metal systems. *Chem. Geol.* 244, 493-506.
- Chang J.S., Law, R., Chang, C.C., 1997. Biosorption of lead, copper and cadmium by biomass of *Pseudomonas aeruginosa* PU21. *Water Res.* 31, 1651–1658.
- Claessens, J., Behrends, T. and van Cappellen, P., 2004. What do acid-base titrations of live bacteria tell us? A preliminary assessment. *Aquat. Sci.* 66, 19-26.
- Claessens, J., van Lith, Y., Laverman, A.M., van Cappellen, P., 2006. Acid-base activity of live bacteria: Implications for quantifying cell wall charge. *Geochim. Cosmochim. Acta* 70, 267-276.
- Cox, J.S., Smith, D.S., Warren, L.A., Ferris, F.G., 1999. Characterizing heterogenous bacterial surface functional groups using discrete affinity spectra for proton binding. *Env. Sci. Tech.* 33, 4514-4521.
- Daughney, C.J., Fein, J.B., 1998. The effect of ionic strength on the adsorption of  $H^+$ ,  $Cd^{2+}$ ,  $Pb^{2+}$ , and  $Cu^{2+}$  by *Bacillus subtilis* and *Bacillus licheniformis*: a surface complexation model. *J. Colloid Interface Sci.* 198, 53-77.
- Daughney, C.J., Fein, J.B., Yee, N., 1998. A comparison of the thermodynamics of metal adsorption onto two common bacteria. *Chem. Geol.* 144, 161-176.
- Daughney, C.J., Fortin, D., 2006. Bacteria and Mineral Interactions. In P. Somasundaran (Ed.) *Encyclopedia of Surface and Colloid Science*, Second Edition, Taylor & Francis, N.Y. pp. 867 - 883.
- Daughney, C.J., Fowle, D.A., Fortin, D.E., 2001. The effect of growth phase on proton and metal adsorption by *Bacillus subtilis*. *Geochim. Cosmochim. Acta* 65(7), 1025–1035.

- Daughney, C.J., Châtellier, X., Chan, A., Kenward, P., Fortin, D., Suttle, C.A., Fowle, D.A., 2004. Adsorption and precipitation of iron from seawater on a marine bacteriophage (PWH3A-P1). *Mar. Chem.* 91, 101–115.
- DeLong, E.F., 1998. Everything in moderation: archaea as 'non-extremophiles'. *Curr. Opin. Genet. Dev.* 8, 649–654.
- DeLong, E.F., Pace, N.R., 2001. Environmental diversity of bacteria and archaea. *Syst. Biol.* 50, 470–478.
- De Rosa, M., Gambacorta, A., Gliozzi, A., 1986. Structure, biosynthesis, and physicochemical properties of archaeobacterial lipids. *Microbiol. Rev.* 50, 70-80.
- Fein, J.B., 2000. Quantifying the effects of bacteria on adsorption reactions in water-rock systems. *Chem. Geol.* 169, 265-280.
- Fein, J.B., Boily, J.-F., Yee, N., Gorman-Lewis, D., Turner, B.F., 2005. Potentiometric titrations of *Bacillus subtilis* cells to low pH and a comparison of modelling approaches. *Geochim. Cosmochim. Acta* 69, 1123-1132.
- Fein, J.B., Daughney, C.J., Yee, N., Davis, T.A., 1997. A chemical equilibrium model for metal adsorption onto bacterial surfaces. *Geochim. Cosmochim. Acta* 61, 3319-3328.
- Fein, J.B., Martin, A.M., Wightman, P.G., 2001. Metal adsorption onto bacterial surfaces: Development of a predictive approach. *Geochim. Cosmochim. Acta* 65, 4267-4273.
- Fernández Murga, M.L., Cabrera, G.M., De Valdez, G.F., Disalvo, A., Seldes, A.M., 2000. Influence of growth temperature on cryotolerance and lipid composition of *Lactobacillus acidophilus*. *J. Appl. Microbiol.* 88, 342-348.

- Fowle, D.A., Fein, J.B., 1999. Competitive adsorption of metal cations onto two Gram-positive bacteria: testing the chemical equilibrium model. *Geochim. Cosmochim. Acta* 63, 3059–3067.
- Fowle, D.A., Fein, J.B., 2000. Experimental measurements of the reversibility of metal–bacteria adsorption reactions. *Chem. Geol.* 168, 27–36.
- Ginn, B.R., Fein, J.B., 2008. The effect of species diversity on metal adsorption onto bacteria. *Geochim. Cosmochim. Acta* 72, 3939–3948.
- Ginn, B., Fein, J.B., 2009. Temperature dependence of Cd and Pb binding onto bacterial cells. *Chem. Geol.* 259, 99–106.
- Gorman-Lewis, D., Fein, J.B., Jensen, M.P., 2006. Enthalpies and entropies of proton and cadmium adsorption onto *Bacillus subtilis* bacterial cells from calorimetric measurements. *Geochim. Cosmochim. Acta* 70, 4862–4873.
- Guiné, V., Martins, J.M.F., Causse, B., Durand, A., Gaudet, J.P., Spadini, L., 2007. Effect of cultivation and experimental conditions on the surface reactivity of the metal-resistant bacteria *Cupriavidus metallidurans* CH34 to protons, cadmium and zinc. *Chem. Geol.* 236, 266–280.
- Haas, J.R., 2004. Effects of cultivation conditions on acid–base titration properties of *Shewanella putrefaciens*. *Chem. Geol.* 209, 67–81.
- Heinrich, H.T.M., Bremer, P.J., Daughney, C.J., McQuillan, A.J., 2007. Acid-base titrations of functional groups on the surface of the thermophilic bacterium *Anoxybacillus flavithermus*: Comparing a chemical equilibrium model with ATR-IR spectroscopic data. *Langmuir* 23, 2731–2740.
- Heinrich, H.T.M., Bremer, P.J., McQuillan, A.J., Daughney, C.J., 2008. Modelling of the acid-base properties of two thermophilic bacteria at different growth times. *Geochim. Cosmochim. Acta* 72, 4185–4200.

- Hershberger, K.L., Barns, S.M., Reysenbach, A.L., Dawson, S.C., Pace, N.R., 1996. Crenarchaeota in low-temperature terrestrial environments. *Nature* 384, 420.
- Hetzer, A., Daughney, C.J., Morgan, H.W., 2006. Cadmium ion biosorption by the thermophilic bacteria *Geobacillus stearothermophilus* and *G. thermocatenulatus*. *Appl. Environ. Microbiol.* 72, 4020–4027.
- Johnson, K.J., Szymanowski, J.E.S., Borrok, D., Huynh, T.Q., Fein, J.B., 2007. Proton and metal adsorption onto bacterial consortia: Stability constants for metal-bacteria surface complexes. *Chem. Geol.* 239, 13-26.
- Klages, K.U., Morgan, H.W., 1994. Characterization of an extremely thermophilic sulphur-metabolising archaebacterium belonging to the Thermococcales. *Arch. Microbiol.* 162, 261-266.
- Koga, Y., Morii, H., 2005. Recent advances in structural research on ether lipids from archaea including comparative and physiological aspects. *Biosci. Biotechnol. Biochem.* 69, 2019–2034.
- Krader, P. and Emerson, D. 2004. Identification of archaea and some extremophilic bacteria using matrix-assisted laser desorption/ionization time-of-flight (MALDI-TOF) mass spectrometry. *Extremophiles* 8, 259-268.
- Kremer, L., Guérardel, Y., Gurcha, S.S., Loch, C., Besra, G.S., 2002. Temperature-induced changes in the cell-wall components of *Mycobacterium thermoresistibile*. *Microbiol.* 148, 3145-3154.
- Kulczycki, E., Ferris, F.G., Fortin, D., 2002. Impact of cell wall structure on the behavior of bacterial cells as sorbents of cadmium and lead. *Geomicrobiol. J.* 19, 553–565.
- Lalonde, S.V., Smith, D.S., Owtrimm, G.W., Konhauser, K.O., 2008. Acid–base properties of cyanobacterial surfaces I: influences of growth phase and

- nitrogen metabolism on cell surface reactivity. *Geochim. Cosmochim. Acta* 72, 1257–1268.
- Langmuir, D., 1997. *Aqueous Environmental Geochemistry*. Prentice Hall, Upper Saddle River, NJ.
- Madigan, M.T., Martinko, J.M. 2005. *Brock Biology of Microorganisms*. 11<sup>th</sup> Edition. Prentice Hall, Upper Saddle River, NJ.
- Ngwenya, B.T., Sutherland, I.W., Kennedy, L., 2003. Comparison of the acid-base behaviour and metal adsorption characteristics of a Gram-negative bacterium with other strains. *Appl. Geochem.* 18, 527–538.
- Özdemir, S., Kilinc, E., Poli, A., Nicolaus, B., Güven, K., 2009. Biosorption of Cd, Cu, Ni, Mn and Zn from aqueous solutions by thermophilic bacteria, *Geobacillus toebii* sub.sp. *decanicus* and *Geobacillus thermoleovorans* sub.sp. *stromboliensis*: Equilibrium, kinetic and thermodynamic studies. *Chem. Eng. J.* 152, 195-206.
- Ronimus, R.S., Reysenbach, A.L., Musgrave, D.R., Morgan, H.W., 1997. The phylogenetic position of the *Thermococcus* isolate AN1 based on 16S rRNA gene sequence analysis: a proposal that AN1 represents a new species, *Thermococcus zilligii* sp. nov. *Arch. Microbiol.* 168, 245-248.
- Smith, R.M., Martell, A.E., 1976. *Critical Stability Constants. IV: Inorganic Complexes*. Plenum, New York, NY.
- Tourney, J., Ngwenya, B.T., Mosselmans, J.W.F., Tetley, L., Cowie, G. L. 2008. The effect of extracellular polymers (EPS) on the proton adsorption characteristics of the thermophile *Bacillus licheniformis* S-86. *Chem. Geol.* 247: 1-15.

- Vetriani, C., Reysenbach, A.L., Doré, J., 1998. Recovery and phylogenetic analysis of archaeal rRNA sequences from continental shelf sediments. *FEMS Microbiol. Lett.* 161, 83-88.
- Westall, J.C., 1982. FITEQL: a computer program for the determination of chemical equilibrium constants from experimental data: Version 1.2, Report 82-01, Department of Chemistry, Oregon State University.
- Westall, J.C., Jones, J.D., Turner, G.D., Zachara, J.M., 1995. Models for association of metal ions with heterogenous environmental sorbents. 1. Complexation of Co(II) by leonardite humic acid as a function of pH and NaClO<sub>4</sub> concentration. *Env. Sci. Tech.* 29: 951-959.
- Wightman, P.G., Fein, J.B., Wesolowski, D.J., Phelps, T.J., Benezeth, P., Palmer, D.A., 2001. Measurement of bacterial surface protonation constants for two species at elevated temperatures. *Geochim. Cosmochim. Acta* 65, 3657–3669.
- Woese, C.R., Fox, G.E., 1977. Phylogenetic structure of the prokaryotic domain: the primary kingdoms. *Proc. Nat. Acad. Sci. USA* 74, 5088-5090.
- Yee, N., Fein, J.B., 2001. Cd adsorption onto bacterial surfaces: A universal adsorption edge?. *Geochim. Cosmochim. Acta* 65, 2037-2042.
- Yee, N., Fein, J.B., 2003. Quantifying metal adsorption onto bacteria mixtures: a test and application of the surface complexation model. *Geomicrobiol. J.* 20, 43–60.
- Yee, N., Fowle, D.A., Ferris, F.G., 2004. A donnan potential model for metal sorption onto *Bacillus subtilis*. *Geochim. Cosmochim. Acta* 68, 3657–3664.

## Figure captions

**Figure 1.** Acid–base titration data (0.01 M) for *T. zilligii*. Error bars are smaller than symbols. (a) Data from four independently prepared cell suspensions, showing that proton adsorption–desorption reactions are reversible and reproducible (symbols of the same shape depict replicate up-pH titrations). (b) Data normalized to biomass concentration. Solid line represents the three-site non-electrostatic model generated by FITMOD when data from all individual titrations are fitted simultaneously.

**Figure 2.** Cd adsorption by a single representative *T. zilligii* cell suspension with biomass concentration varied by dilution with the electrolyte (total Cd =  $5 \times 10^{-5}$  M, ionic strength = 0.01 M). Error bars represent  $2\sigma$  uncertainties. Solid line represents model fit to the experimental data.

**Figure 3.** Comparison of proton adsorption by thermophiles and mesophiles at ionic strength 0.01 M. Dashed line represents the universal model curve for mesophilic bacteria, with shaded area representing  $\pm 1\sigma$  around the average (Borrok et al., 2005). Solid lines show model curves for various thermophiles, labelled by abbreviations at right: Tz = *Thermococcus zilligii* (this study); Gt = *Geobacillus thermocatenulatus* (Hetzer et al., 2006); Af = *Anoxybacillus flavithermus* (Burnett et al., 2006a; Heinrich et al., 2007); TOR-39 = a thermophilic bacterium similar to *Thermoanaerobacter ethanolicus* (Wightman et al., 2001); Tt = *Thermus thermophilus* (Ginn and Fein, 2008); Gs = *Geobacillus stearothermophilus* (Heinrich et al., 2008). \* denotes model curves for populations in exponential phase.

**Figure 4.** Total proton buffering capacity as a function of growth temperature for different species over the pH range 4 to 10, at biomass concentration of 1 wet g per litre and ionic strength 0.01. Data points are labelled as follows: Univ-J, Univ-B and Univ-Y represent universal models for mesophilic bacteria and consortia, with  $\pm 1\sigma$  around the average, based on Johnson et al. (2007), Borrok et al. (2005) and Yee and Fein (2001), respectively; Tz = *Thermococcus zilligii* (this study); Gt = *Geobacillus thermocatenulatus* (Hetzer et al., 2006); Af = *Anoxybacillus flavithermus* (Burnett et al., 2006a; Heinrich et al., 2007); TOR-39 = a thermophilic bacterium similar to *Thermoanaerobacter ethanolicus* (Wightman et al., 2001); Tt = *Thermus thermophilus* (Ginn and Fein, 2008); Gs = *Geobacillus stearothermophilus* (Heinrich et al., 2008). \* denotes populations in exponential phase.

**Figure 5.** Comparison of Cd adsorption by thermophiles and mesophiles for biomass concentration of 1 wet g per litre, total Cd concentration of  $5 \times 10^{-5}$  M and ionic strength 0.01 M. Dashed line represents the universal model curve for mesophilic bacteria, with shaded area representing  $\pm 1\sigma$  around the average (Yee and Fein, 2001). Solid lines show model curves for various thermophiles, labelled by abbreviations at right: Tz = *Thermococcus zilligii* (this study); Gt = *Geobacillus thermocatenulatus* (Hetzer et al., 2006); Tt = *Thermus thermophilus* (Ginn and Fein, 2008); Gs = *Geobacillus stearothermophilus* (Hetzer et al., 2006); Af = *Anoxybacillus flavithermus* (Burnett et al., 2006b). \* denotes model curves for populations in exponential phase.

**Figure 6.** Total Cd adsorption as a function of growth temperature for different species at pH 6, biomass concentration of 1 wet g per litre, total Cd concentration of 5



$\times 10^{-5}$  M and ionic strength 0.01 M. Data points are labelled as follows: Univ-J and Univ-Y represent universal models for mesophilic bacteria and consortia, with  $\pm 1\sigma$  around the average, based on Johnson et al. (2007) and Yee and Fein (2001), respectively; Tz = *Thermococcus zilligii* (this study); Gt = *Geobacillus thermocatenulatus* (Hetzer et al., 2006); Af = *Anoxybacillus flavithermus* (Burnett et al., 2006b); Gs = *Geobacillus stearothermophilus* (Hetzer et al., 2006); Tt = *Thermus thermophilus* (Ginn and Fein, 2008); \* denotes populations in exponential phase.

1 **Table 1.** Parameters for non-electrostatic surface complexation models describing acid–base titrations of *T. zilligii*.

| Trial <sup>a</sup> | n <sup>b</sup> | Model      | pK <sub>a</sub> values <sup>c</sup> |        |        |        | Site Concentrations <sup>d</sup> |        |        |        | Model Fit <sup>e</sup> |      |       |       |
|--------------------|----------------|------------|-------------------------------------|--------|--------|--------|----------------------------------|--------|--------|--------|------------------------|------|-------|-------|
|                    |                |            | Site 1                              | Site 2 | Site 3 | Site 4 | Site 1                           | Site 2 | Site 3 | Site 4 | Total                  | V(Y) | Lower | Upper |
| 1                  | 93             | two-site   | 5.04                                | 8.51   | -      | -      | 2.81                             | 2.76   | -      | -      | 5.57                   | 27.6 | 21.0  | 38.0  |
|                    |                | three-site | 4.86                                | 6.84   | 9.13   | -      | 2.51                             | 0.98   | 3.10   | -      | 6.58                   | 20.7 | 15.7  | 28.6  |
|                    |                | four-site  | 4.82                                | 6.48   | 8.27   | 9.82   | 1.83                             | 0.60   | 0.85   | 3.16   | 6.44                   | 20.3 | 15.4  | 28.1  |
| 2                  | 74             | two-site   | 4.86                                | 8.11   | -      | -      | 3.49                             | 2.30   | -      | -      | 5.79                   | 14.1 | 10.4  | 20.4  |
|                    |                | three-site | 4.46                                | 6.12   | 8.94   | -      | 0.89                             | 0.57   | 0.77   | -      | 2.23                   | 6.8  | 5.0   | 9.8   |
|                    |                | four-site  | -----                               |        |        |        | No convergence                   |        |        |        | -----                  |      |       |       |
| 3                  | 94             | two-site   | 4.77                                | 7.67   | -      | -      | 3.47                             | 1.51   | -      | -      | 4.99                   | 11.4 | 8.7   | 15.7  |
|                    |                | three-site | -----                               |        |        |        | No convergence                   |        |        |        | -----                  |      |       |       |
|                    |                | four-site  | -----                               |        |        |        | No convergence                   |        |        |        | -----                  |      |       |       |
| 4                  | 97             | two-site   | 4.79                                | 7.68   | -      | -      | 2.85                             | 1.65   | -      | -      | 4.50                   | 9.0  | 6.9   | 12.3  |
|                    |                | three-site | 4.54                                | 6.28   | 8.86   | -      | 1.65                             | 0.86   | 1.09   | -      | 3.60                   | 4.6  | 3.5   | 6.3   |
|                    |                | four-site  | -----                               |        |        |        | No convergence                   |        |        |        | -----                  |      |       |       |
| All                | 358            | two-site   | 4.95                                | 8.17   |        |        | 3.05                             | 1.95   |        |        | 5.00                   | 20.5 | 17.8  | 23.9  |
|                    |                | three-site | 4.60                                | 6.26   | 8.96   |        | 2.50                             | 1.30   | 2.09   |        | 5.89                   | 13.6 | 11.8  | 15.8  |
|                    |                | four-site  | 4.47                                | 5.78   | 7.74   | 9.73   | 2.21                             | 1.35   | 0.86   | 3.06   | 7.48                   | 12.7 | 11.0  | 14.8  |

2

3 <sup>a</sup> Trials 1 to 4 pertain to individually cultured cell suspensions that were modelled independently. All describes the model simultaneously fit to  
4 data from the four individual trials.

5 <sup>b</sup> Number of data points in each dataset. Trials 1 to 4 involve titrations of two independent aliquots of cell suspension, each of which was titrated  
6 twice in the up-pH direction.

7 <sup>c</sup> Negative logarithm of stability constants for deprotonation of surface sites (Equations 1 and 3), referenced to zero ionic strength and 25°C.

8 <sup>d</sup> Concentrations of surface sites in  $\times 10^{-5}$  moles per gram wet biomass.

9 <sup>e</sup> V(Y) is the variance calculated by FITMOD; Lower and Upper represent 95% confidence intervals (Equation 6).

10 **Table 2.** Parameters for three-site non-electrostatic surface complexation models describing adsorption of Cd by *T. zilligii*.

| Trial <sup>a</sup> | n <sup>b</sup> | Log <i>K</i> values <sup>c</sup> |        |        | Model Fit <sup>d</sup> |       |       |
|--------------------|----------------|----------------------------------|--------|--------|------------------------|-------|-------|
|                    |                | Site 1                           | Site 2 | Site 3 | V(Y)                   | Lower | Upper |
| 1                  | 22             | 4.10                             | -      | -      | 2.2                    | 1.3   | 4.4   |
|                    |                | -                                | 4.60   | -      | 9.8                    | 5.8   | 20.0  |
|                    |                | -                                | -      | 5.69   | 19.2                   | 11.3  | 39.1  |
| 2                  | 27             | 3.91                             | -      | -      | 5.5                    | 3.4   | 10.3  |
|                    |                | -                                | 4.42   | -      | 16.0                   | 9.9   | 30.0  |
|                    |                | -                                | -      | 5.56   | 26.7                   | 16.5  | 50.0  |
| 3                  | 28             | 3.87                             | -      | -      | 3.3                    | 2.1   | 6.1   |
|                    |                | -                                | 4.37   | -      | 15.2                   | 9.5   | 28.1  |
|                    |                | -                                | -      | 5.71   | 29.8                   | 18.6  | 55.2  |
| 4                  | 25             | 4.04                             | -      | -      | 4.3                    | 2.6   | 8.3   |
|                    |                | -                                | 4.73   | -      | 10.0                   | 6.1   | 19.4  |
|                    |                | -                                | -      | 6.74   | 15.9                   | 9.7   | 30.7  |
| All                | 102            | 3.95                             | -      | -      | 4.3                    | 3.3   | 5.8   |
|                    |                | -                                | 4.52   | -      | 13.3                   | 10.3  | 17.9  |
|                    |                | -                                | -      | 6.13   | 25.1                   | 19.4  | 33.7  |

11

12 <sup>a</sup> Trials 1 to 4 pertain to individually cultured cell suspensions that were modelled independently. All describes the model simultaneously fit to  
 13 data from the four individual trials.

14 <sup>b</sup> Number of data points in each dataset.

15 <sup>c</sup> Log *K* values describing adsorption of Cd onto one of the three types of surface sites incorporated into the model (Equations 2 and 4). Sites  
 16 have p*K*<sub>a</sub> values and concentrations as specified by the three-site “All” model in Table 1. Models that consider Cd adsorption onto any  
 17 combination of two or three different types of surface sites fail to converge.

18 <sup>d</sup> V(Y) is the variance calculated by FITMOD; Lower and Upper represent 95% confidence intervals (Equation 6).

19 **Table 3.** Three-site non-electrostatic models (Equations 1 to 4) fitted to data from previous investigations.

| Reference      | Species <sup>a</sup>     | °C <sup>b</sup>                         | pK <sub>a</sub> values |        |        | Site Concentrations |        |        |       | Cd log K values |        |        |      |
|----------------|--------------------------|---|------------------------|--------|--------|---------------------|--------|--------|-------|-----------------|--------|--------|------|
|                |                          |   | Site 1                 | Site 2 | Site 3 | Site 1              | Site 2 | Site 3 | Total | Site 1          | Site 2 | Site 3 |      |
| Thermophiles   | This study               | <i>Thermococcus zilligii</i> *          | 75                     | 4.60   | 6.26   | 8.96                | 2.50   | 1.30   | 2.09  | 5.89            | 3.95   | -      | -    |
|                | Wightman et al. (2001)   | TOR-39                                  | 55                     | 4.59   | 5.95   | 8.42                | 6.04   | 4.93   | 3.08  | 14.05           | -      | -      | -    |
|                | Burnett et al. (2006a,b) | <i>Anoxybacillus flavithermus</i>       | 60                     | 4.77   | 6.10   | 8.13                | 5.05   | 3.66   | 3.86  | 12.56           | 3.12   | 3.49   | 6.08 |
|                | Heinrich et al. (2007)   | <i>Anoxybacillus flavithermus</i> *     | 57                     | 3.03   | 5.25   | 8.07                | 9.51   | 16.12  | 7.13  | 32.76           | -      | -      | -    |
|                | Heinrich et al. (2008)   | <i>Geobacillus stearothermophilus</i>   | 57                     | 3.15   | 5.92   | 7.04                | 2.54   | 4.13   | 8.19  | 14.86           | -      | -      | -    |
|                | Heinrich et al. (2008)   | <i>Geobacillus stearothermophilus</i> * | 57                     | 2.31   | 4.34   | 6.88                | 19.21  | 17.85  | 12.76 | 49.82           | -      | -      | -    |
|                | Hetzer et al. (2007)     | <i>Geobacillus thermocatenulatus</i>    | 60                     | 4.12   | 5.47   | 8.09                | 3.27   | 6.27   | 2.42  | 11.96           | 3.72   | 3.96   | 4.34 |
|                | Ginn and Fein (2008)     | <i>Thermus thermophilus</i>             | 80                     | 3.75   | 5.73   | 8.81                | 11.18  | 4.47   | 3.08  | 18.73           | 2.72   | 3.78   | 5.23 |
| Mesophiles     | Borrok et al. (2005)     | Universal, 36 species/consortia         | 37                     | 3.72   | 5.90   | 8.74                | 16.68  | 7.64   | 7.05  | 31.37           | -      | -      | -    |
|                |                          | Universal - 1σ                          | 37                     | 4.06   | 6.23   | 8.83                | 8.14   | 3.97   | 3.69  | 15.79           | -      | -      | -    |
|                |                          | Universal + 1σ                          | 37                     | 3.59   | 5.77   | 8.69                | 25.11  | 11.45  | 10.34 | 46.90           | -      | -      | -    |
|                | Johnson et al. (2007)    | Universal, 3 consortia                  | 25                     | 3.85   | 5.76   | 8.99                | 17.14  | 10.76  | 9.79  | 37.69           | 3.25   | 3.97   | 5.73 |
|                |                          | Universal - 1σ                          | 25                     | 3.95   | 5.86   | 9.02                | 13.71  | 8.31   | 7.76  | 29.78           | 2.89   | 3.67   | 4.80 |
|                |                          | Universal + 1σ                          | 25                     | 3.77   | 5.70   | 8.97                | 20.51  | 13.25  | 11.82 | 45.58           | 3.45   | 4.09   | 6.01 |
|                | Yee and Fein (2001)      | Universal, 9 species                    | 32                     | 5.12   | 7.38   | 10.44               | 18.77  | 8.63   | 46.28 | 73.68           | 4.05   | 4.56   | 4.96 |
|                |                          | Universal - 1σ                          | 32                     | 5.11   | 7.36   | 11.38               | 11.65  | 4.72   | 48.61 | 64.98           | 3.70   | 3.75   | 5.18 |
| Universal + 1σ |                          | 32                                      | 5.13                   | 7.36   | 10.15  | 25.58               | 12.66  | 34.46  | 72.70 | 4.31            | 5.48   | 4.14   |      |

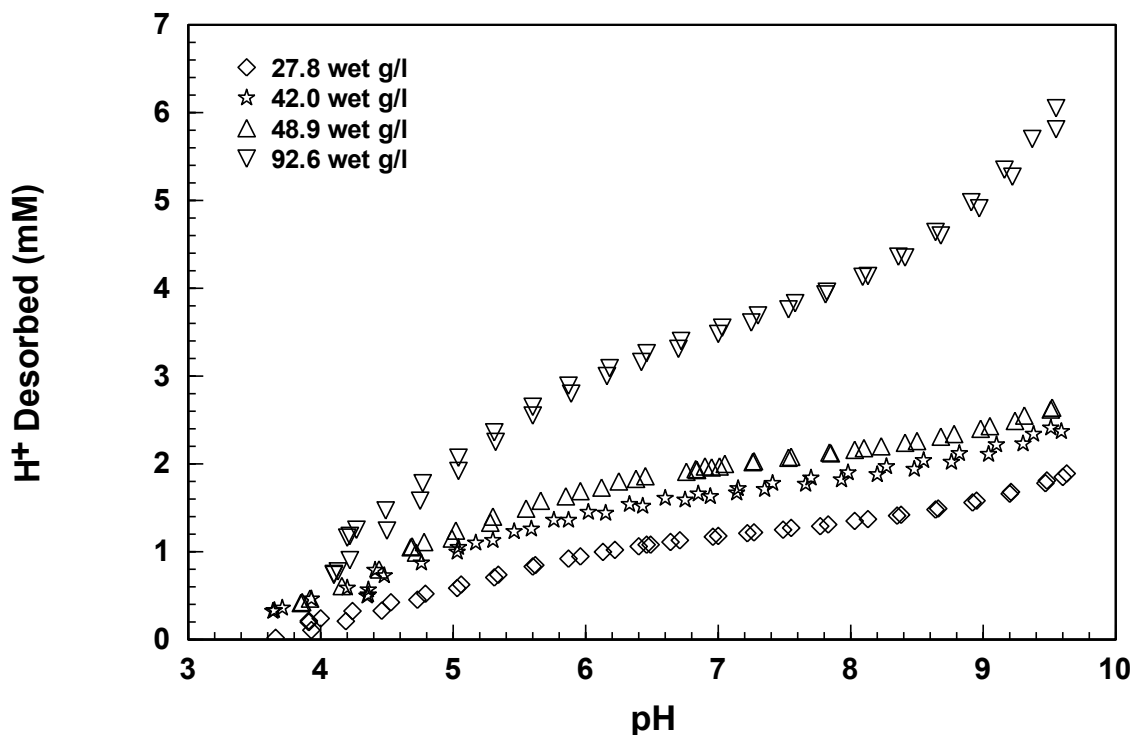
20

21 <sup>a</sup> Individual species for thermophiles (\* denotes populations in exponential phase; all other populations are in stationary/death phase, or growth  
 22 phase was not reported). Individual “universal” models for mesophiles are re-developed for the average, the average - 1 standard deviation, and  
 23 the average + 1 standard deviation, based on uncertainties reported in previous studies.

24 <sup>b</sup> Growth temperature.

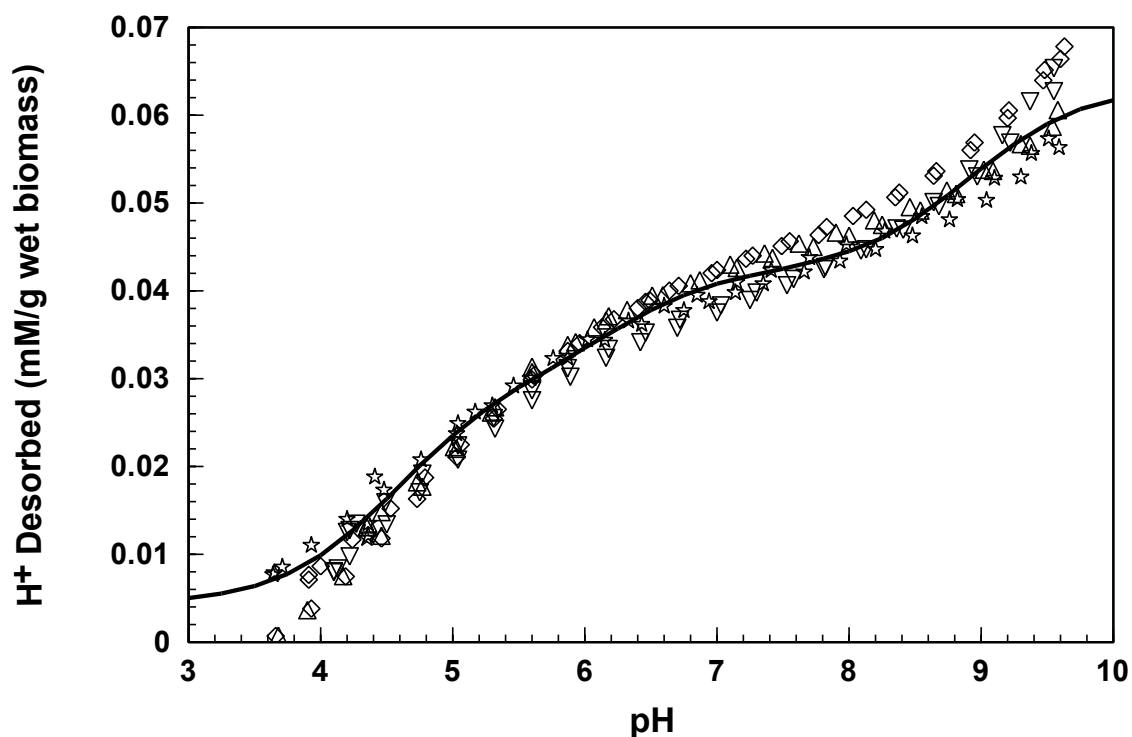
25 **Figure 1.** Acid–base titration data (0.01 M) for *T. zilligii*. Error bars are smaller than  
26 symbols. (a) Data from four independently prepared cell suspensions, showing that  
27 proton adsorption–desorption reactions are reversible and reproducible (symbols of  
28 the same shape depict replicate up-pH titrations). (b) Data normalized to biomass  
29 concentration. Solid line represents the three-site non-electrostatic model generated  
30 by FITMOD when data from all individual titrations are fitted simultaneously.  
31  
32

a)



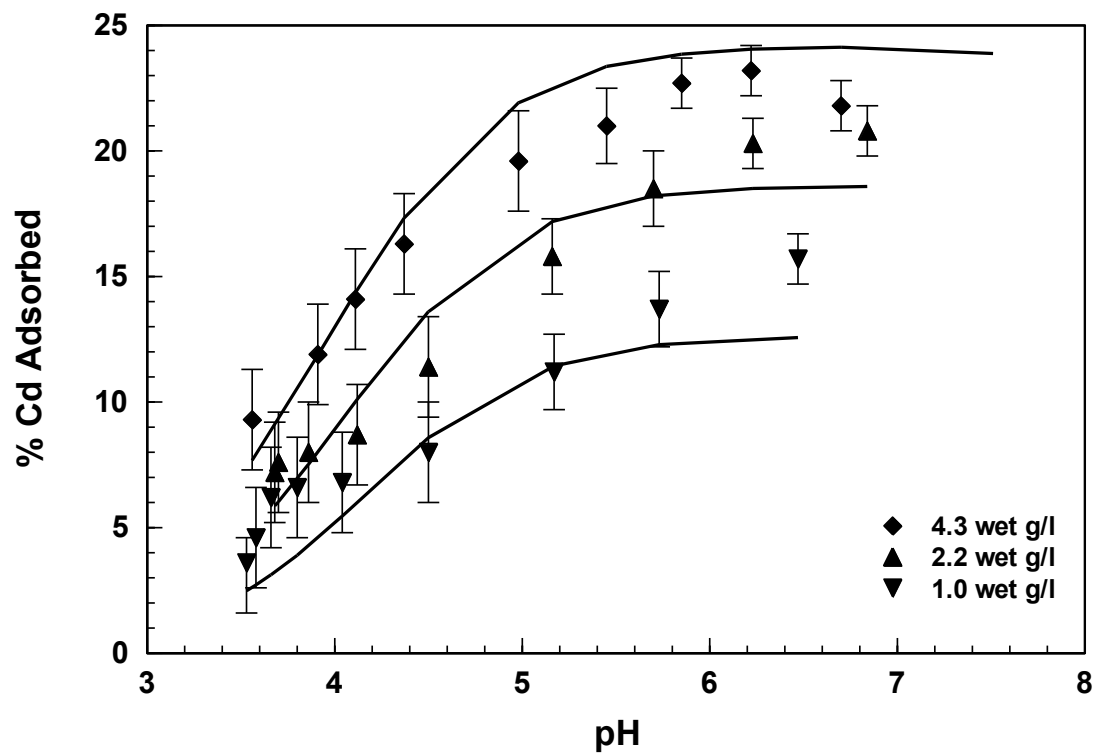
33  
34

b)



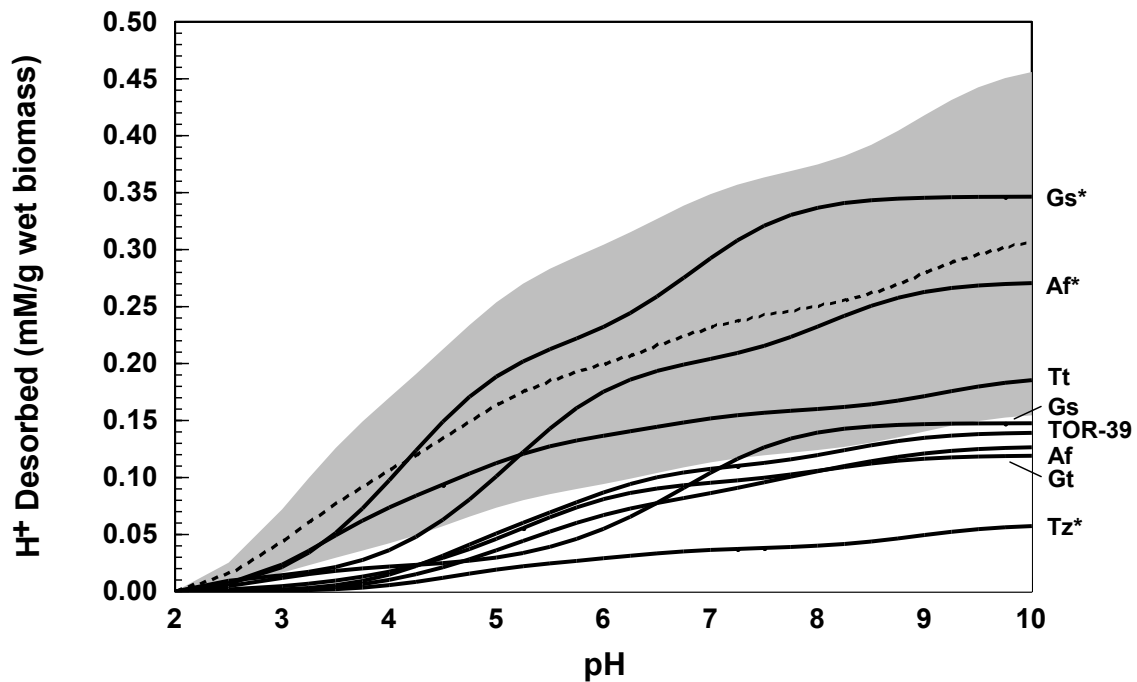
35  
36

37 **Figure 2.** Cd adsorption by a single representative *T. zilligii* cell suspension with  
38 biomass concentration varied by dilution with the electrolyte (total Cd =  $5 \times 10^{-5}$  M,  
39 ionic strength = 0.01 M). Error bars represent  $2\sigma$  uncertainties. Solid line represents  
40 model fit to the experimental data.  
41  
42



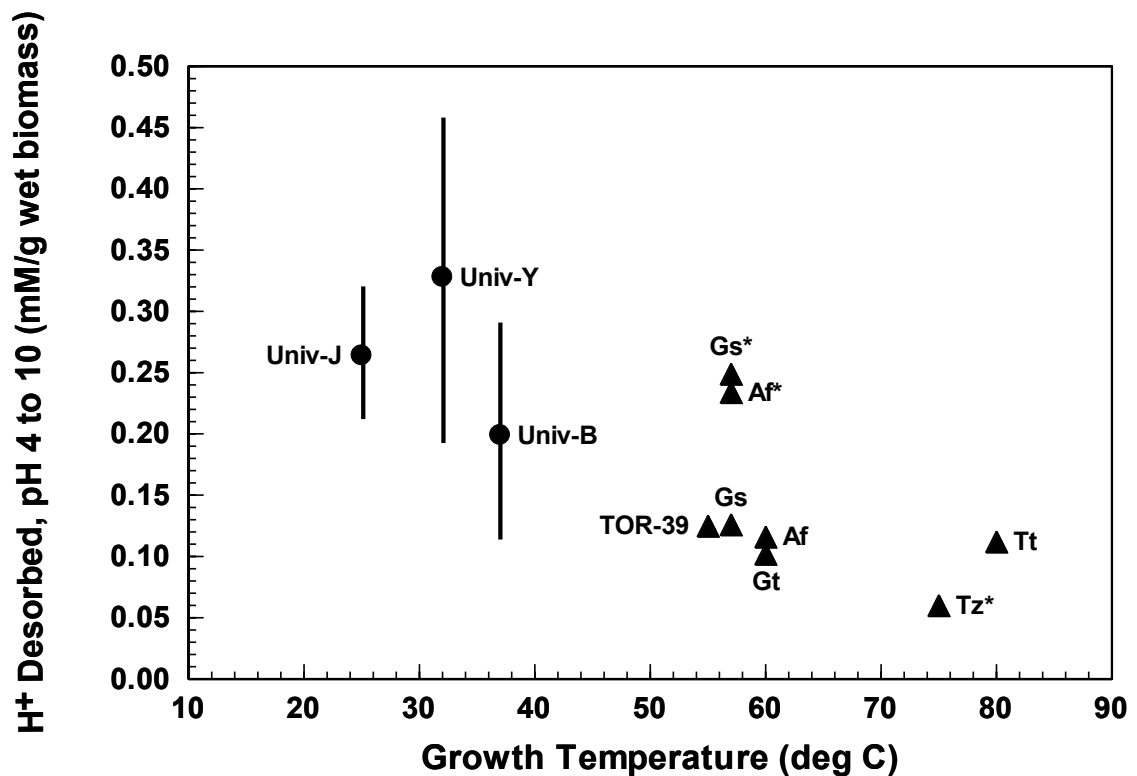
43  
44

45 **Figure 3.** Comparison of proton adsorption by thermophiles and mesophiles at ionic  
 46 strength 0.01 M. Dashed line represents the universal model curve for mesophilic  
 47 bacteria, with shaded area representing  $\pm 1\sigma$  around the average (Borrok et al., 2005).  
 48 Solid lines show model curves for various thermophiles, labelled by abbreviations at  
 49 right: Tz = *Thermococcus zilligii* (this study); Gt = *Geobacillus thermocatenulatus*  
 50 (Hetzer et al., 2006); Af = *Anoxybacillus flavithermus* (Burnett et al., 2006a; Heinrich  
 51 et al., 2007); TOR-39 = a thermophilic bacterium similar to *Thermoanaerobacter*  
 52 *ethanolicus* (Wightman et al., 2001); Tt = *Thermus thermophilus* (Ginn and Fein,  
 53 2008); Gs = *Geobacillus stearothermophilus* (Heinrich et al., 2008). \* denotes model  
 54 curves for populations in exponential phase.  
 55



56  
 57

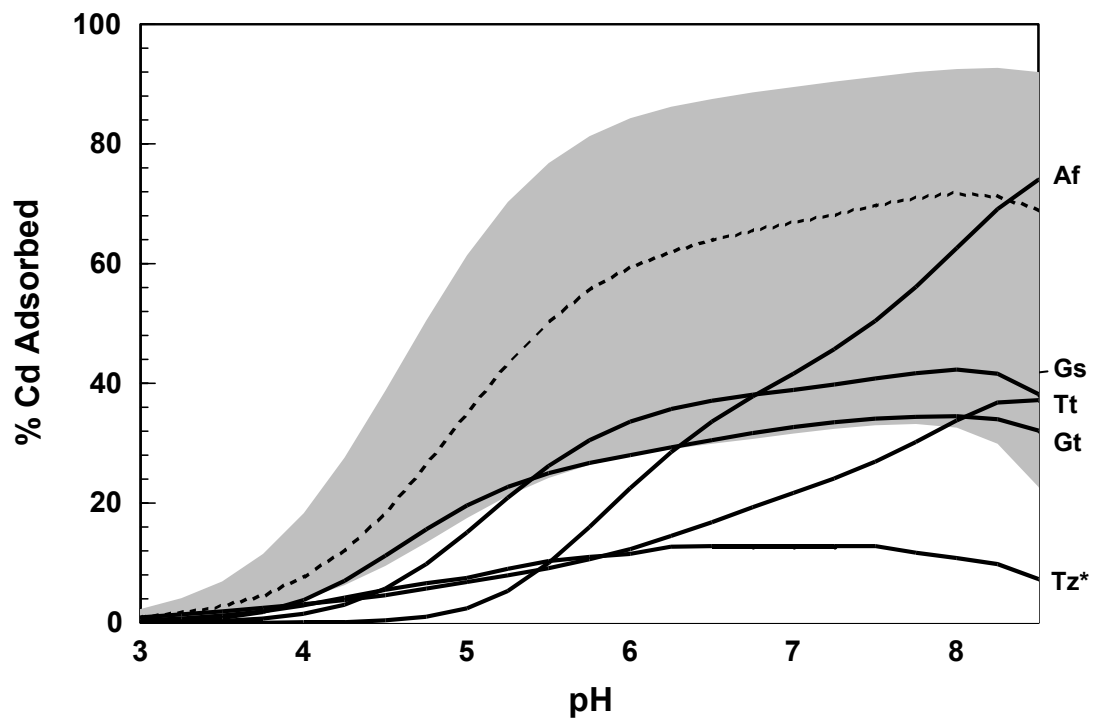
58 **Figure 4.** Total proton buffering capacity as a function of growth temperature for  
 59 different species over the pH range 4 to 10, at biomass concentration of 1 wet g per  
 60 litre and ionic strength 0.01. Data points are labelled as follows: Univ-J, Univ-B and  
 61 Univ-Y represent universal models for mesophilic bacteria and consortia, with  $\pm 1\sigma$   
 62 around the average, based on Johnson et al. (2007), Borrok et al. (2005) and Yee and  
 63 Fein (2001), respectively; Tz = *Thermococcus zilligii* (this study); Gt = *Geobacillus*  
 64 *thermocatenulatus* (Hetzer et al., 2006); Af = *Anoxybacillus flavithermus* (Burnett et  
 65 al., 2006a; Heinrich et al., 2007); TOR-39 = a thermophilic bacterium similar to  
 66 *Thermoanarobacter ethanolicus* (Wightman et al., 2001); Tt = *Thermus thermophilus*  
 67 (Ginn and Fein, 2008); Gs = *Geobacillus stearothermophilus* (Heinrich et al., 2008). \*  
 68 denotes populations in exponential phase.  
 69  
 70



71  
 72



73 **Figure 5.** Comparison of Cd adsorption by thermophiles and mesophiles for biomass  
 74 concentration of 1 wet g per litre, total Cd concentration of  $5 \times 10^{-5}$  M and ionic  
 75 strength 0.01 M. Dashed line represents the universal model curve for mesophilic  
 76 bacteria, with shaded area representing  $\pm 1\sigma$  around the average (Yee and Fein, 2001).  
 77 Solid lines show model curves for various thermophiles, labelled by abbreviations at  
 78 right: Tz = *Thermococcus zilligii* (this study); Gt = *Geobacillus thermocatenulatus*  
 79 (Hetzer et al., 2006); Tt = *Thermus thermophilus* (Ginn and Fein, 2008); Gs =  
 80 *Geobacillus stearothermophilus* (Hetzer et al., 2006); Af = *Anoxybacillus*  
 81 *flavithermus* (Burnett et al., 2006b). \* denotes model curves for populations in  
 82 exponential phase.  
 83



84  
 85

86 **Figure 6.** Total Cd adsorption as a function of growth temperature for different  
 87 species at pH 6, biomass concentration of 1 wet g per litre, total Cd concentration of  $5$   
 88  $\times 10^{-5}$  M and ionic strength 0.01 M. Data points are labelled as follows: Univ-J and  
 89 Univ-Y represent universal models for mesophilic bacteria and consortia, with  $\pm 1\sigma$   
 90 around the average, based on Johnson et al. (2007) and Yee and Fein (2001),  
 91 respectively; Tz = *Thermococcus zilligii* (this study); Gt = *Geobacillus*  
 92 *thermocatenulatus* (Hetzer et al., 2006); Af = *Anoxybacillus flavithermus* (Burnett et  
 93 al., 2006b); Gs = *Geobacillus stearothermophilus* (Hetzer et al., 2006); Tt = *Thermus*  
 94 *thermophilus* (Ginn and Fein, 2008); \* denotes populations in exponential phase.

95  
 96

